THE JOURNAL OF BIOLOGICAL CHEMISTRY VOL. 286, NO. 20, pp. 18190–18201, May 20, 2011
Printed in the U.S.A.

Spatial Phosphoprotein Profiling Reveals a Compartmentalized Extracellular Signal-regulated Kinase Switch Governing Neurite Growth and Retraction*[S]

Received for publication, March 2, 2011, and in revised form, March 24, 2011 Published, JBC Papers in Press, March 28, 2011, DOI 10.1074/jbc.M111.236133

Yingchun Wang[‡§1,2], Feng Yang[¶1], Yi Fu[§], Xiahe Huang[§], Wei Wang[‡§], Xinning Jiang[‡], Marina A. Gritsenko[¶], Rui Zhao[¶], Matthew E. Monore[¶], Olivier C. Pertz[‡3], Samuel O. Purvine[¶], Daniel J. Orton[¶], Jon M. Jacobs[¶], David G. Camp II[¶], Richard D. Smith[¶], and Richard L. Klemke[‡4]

From the [‡]Department of Pathology and Moores Cancer Center, University of California, San Diego, La Jolla, California 92093, the [¶]Biological Sciences Division, Environmental Molecular Sciences Laboratory, Pacific Northwest National Laboratory, Richland, Washington 99354, and the [§]State Key Laboratory of Molecular and Developmental Biology, Institute of Genetics and Developmental Biology, Chinese Academy of Sciences, Beijing, 100101, China

Brain development and spinal cord regeneration require neurite sprouting and growth cone navigation in response to extension and collapsing factors present in the extracellular environment. These external guidance cues control neurite growth cone extension and retraction processes through intracellular protein phosphorylation of numerous cytoskeletal, adhesion, and polarity complex signaling proteins. However, the complex kinase/substrate signaling networks that mediate neuritogenesis have not been investigated. Here, we compare the neurite phosphoproteome under growth and retraction conditions using neurite purification methodology combined with mass spectrometry. More than 4000 non-redundant phosphorylation sites from 1883 proteins have been annotated and mapped to signaling pathways that control kinase/phosphatase networks, cytoskeleton remodeling, and axon/dendrite specification. Comprehensive informatics and functional studies revealed a compartmentalized ERK activation/deactivation cytoskeletal switch that governs neurite growth and retraction, respectively. Our findings provide the first system-wide analysis of the phosphoprotein signaling networks that enable neurite growth and retraction and reveal an important molecular switch that governs neuritogenesis.

Neuritogenesis is a dynamic process involving the extension of long, thin protrusions called neurites that will subsequently differentiate into long axons or an elaborate dendritic arbor (1–4). This highly polarized process occurs through the segmentation from the soma periphery of a microtubule-rich shaft capped with a growth cone, which itself is characterized by an actin-rich lamellipodium with numerous filopodial extensions and integrin-mediated adhesive contacts. Understanding this process is crucial, as it is necessary for proper wiring of the brain and nerve regeneration and has been linked to numerous neurodegenerative diseases.

Although cultured neurons randomly form neurites *in vitro*, *in vivo* this process is orchestrated by gradients of chemoattractants, extracellular matrix proteins, and collapsing factors that precisely guide neurite initiation and advancement (5, 6). This occurs in a polarized and highly controlled manner and relies on spatially regulated mechanisms for gradient sensing, membrane trafficking, integrin-mediated adhesion, and organization of the actin-microtubule cytoskeleton (5–8). These events are largely orchestrated by numerous surface guidance/repulsion and adhesion receptors that signal to the cell interior through multiple kinase activation and substrate phosphorylation events (7, 9–17). Protein phosphorylation is a critical post-translational modification that regulates protein-protein interactions, enzymatic activity, and subcellular localization. The reversible addition of PO_4^{3-} to serine, threonine, and tyrosine amino acid residues is mediated by more than 500 kinases and more than 150 phosphatases (18–20). In many cases, kinases phosphorylate specific amino acids in the context of a consensus recognition sequence. For example, ERK is a proline-directed kinase that phosphorylates Ser/Thr residues with the consensus sequence P*X*(S/T)P, where *X* can be a neutral or basic amino acid (21–24). The identification of phosphorylation sites in the context of a specific kinase recognition sequence of given substrates has proven quite useful in the predication of kinase activation events in the cell (25–27). Also, kinases themselves can be phosphorylated at specific sites that are known to promote enzymatic activation, which can be used to predict kinase activity in the cell. This is further enriched by computational models that predict higher order contextual features of kinases such as protein scaffolding, subcellular localization, and expression patterns (13, 25–28). When combined, *in silico* programs have been shown to predict kinase activity with significant accuracy. This approach has been applied to large phosphoproteomic data sets consisting of thousands of phosphorylation sites revealing important kinase signaling networks

* This work was supported, in whole or in part, by National Institutes of Health Grants GM068487 (to R. L. K.), CA097022 (to R. L. K.), and RR018522 (to R. D. S.).
[S] The on-line version of this article (available at http://www.jbc.org) contains supplemental Tables 1–3 and Fig. 1.
[1] Both authors contributed equally to this work.
[2] Supported by the One Hundred Talents project of the Chinese Academy of Sciences.
[3] Present address: Institute of Biochemistry and Genetics, Dept. of Biomedicine, University of Basal, CH-4003 Basel, Switzerland.
[4] To whom correspondence should be addressed: Dept. of Pathology and Moores Cancer Center, University of California, San Diego, Basic Science Bldg. 1040, 9500 Gilman Dr., MC 0612, La Jolla, CA 92093. Tel.: 858-822-5610; Fax: 858-822-4566; E-mail: rklemke@ucsd.edu.

that modulate cell migration, DNA damage, and yeast biology (13, 25, 29, 30).

Although significant progress has been made in identifying specific signals regulating neuritogenesis, a system-wide analysis of the phosphoprotein signals that control this process has not been investigated. Consequently, our understanding of the complex kinase/substrate signaling networks that regulate neurite formation and guidance is not defined. Here we describe a microporous filter method that facilitates selective purification of neurites undergoing growth or retraction. This fractionation method combined with immobilized metal-ion affinity chromatography and LC-MS protein identification technologies facilitated the identification of thousands of protein phosphorylation signatures that mediate neurite extension or retraction events induced by growth promoting or collapsing stimuli, respectively. Functional annotation and kinase activity predications *in silico* revealed phosphoprotein networks controlling cytoskeletal remodeling, axon/dendrite specification, and cell adhesion. Kinase signaling analysis and cell-based assays revealed that an integrin/MEK/ERK signaling pathway operates as a critical switch controlling neurite extension and retraction dynamics.

EXPERIMENTAL PROCEDURES

Antibodies and Reagents—Lysophosphatidic acid was from Sigma. ROCK[5] inhibitor Y-27632 was from Sigma, and ERK kinase inhibitor PD98059 was from Calbiochem. Alexa-fluor 488-labeled phalloidin was from Invitrogen. DM-1A anti-α-tubulin antibodies and Alexa-fluor 546-conjugated secondary antibodies were from Sigma. C14 anti-ERK antibody was from Santa Cruz. Anti-p130CAS was from Cell Signaling or Santa Cruz. Anti-Cdc42 and -Rac antibodies were from Millipore. Phospho-MEK1 Ser-298 and Thr-292 and anti-phospho-ERK-TEY antibodies were from BIOSOURCE. Anti-MEK1 and Crk antibody were from BD Transduction Laboratories. Phospho-MEK1/2 Ser-218/Ser-222 antibody was from Cell Signaling. Anti-myosin light chain and anti-phospho-myosin light chain serine 19 antibodies were from Sigma. Anti-Akt and anti-phospho-Akt-S473 were from Cell Signaling. Anti-phosphotyrosine 4G10 was from Millipore. Anti-Abl kinase antibody was from Sigma. Anti-FAK was from Santa Cruz, and anti-phospho-FAK-Y397 antibody was from BIOSOURCE. All MEK constructs have been previously described and were kindly provided by Dr. Andrew Catling (Louisiana State University Health Sciences Center, New Orleans, LA) (31–34).

Purification of Growing and Retracting Neurites—Procedures for the culturing and biochemical preparation of extending neurites from NIE-115 cells using 3.0-μm microporous filters were the same as described before (35). To purify retracting neurites, NIE-115 cells were allowed to extend neurites for various times (8–24 h) toward laminin (10 μg/ml, Millipore), then LPA (1 μM) was added to the media in either the upper or lower chamber to induce retraction for the times indicated in the text. Extending or retracting neurites or their corresponding cell bodies were differentially harvested into lysis buffer for biochemical analyses as described (35). For GTPase activity assays, lysates were prepared as previously described (35). To block LPA-induced neurite retraction 10 μM Y-27632 was added to the chamber for 60 min before LPA stimulation. To block ERK activation, 25 μM PD98059 was added to the chamber for the indicated times. Transient transfection of NIE-115 with the plasmids, neurite imaging, and immunofluorescence of the neurite cytoskeleton was performed as described (35). To prepare samples for proteomics analysis, extending or retracting neurites or their corresponding cell bodies were differentially harvested into lysis buffer of freshly made 7 M urea, 0.5% Nonidet P-40 in 50 mM ammonium bicarbonate (pH 8.0) containing 50 nM calyculin A and 0.2 mM vanadate as phosphatase inhibitors. After incubation on ice for 30 min, insoluble matter was removed by centrifugation at 16,000 × *g* for 20 min.

Phosphopeptide Enrichment and Capillary HPLC-MS/MS Analysis—Protein samples (five biological replicates each for both extending and retracting neurites) were digested with trypsin at room temperature. Tryptic peptides were desalted and methyl-esterified (250 μg for each sample) followed by immobilized metal-ion (Fe^{3+}) affinity chromatography to enrich phosphopeptides, as detailed in a recent report (36). After immobilized metal-ion affinity chromatography enrichment, aliquots (one-sixth of the immobilized metal-ion affinity chromatography elution) were analyzed on a ThermoElectron LTQ-Orbitrap (Waltham, MA) coupled to an automated dual-column phosphoproteome nano-HPLC platform assembled in-house. The LC gradient (A = 100 mM HOAc in H_2O, B = 70% acetonitrile, 100 mM HOAc in H_2O) was 0–70% B for ~180 min. For each sample, two technical replicates of LC-MS analyses were performed (36).

Data Base Search and Peptide Identification—Phosphopeptides were identified from MS/MS spectra using SEQUEST by searching against the mouse IPI data base. For confident phosphopeptide identifications, the false discovery rate at peptide spectrum level was controlled at ≤0.5% using in-house developed software (37). This program also measured the probability of correct phosphorylation site localization in each identified peptide by calculating the AScore for each phosphorylation site (38), and the assigned top phosphopeptide sequence was taken as the final peptide identification for a given spectrum.

Evaluation of Phosphopeptide Changes in Growth and Retracting Neurite—We applied the spectral count method to evaluate the changes of phosphopeptides. The total spectral counts for each identified phosphopeptide in each neurite condition and their ratios were used to semi-quantitatively estimate their abundance in each condition (39).

Bioinformatics—The pathway analysis was performed using the Ingenuity Pathway Analysis software (Ingenuity Systems) as previously described (48). Briefly, we queried all phosphoproteins against the Ingenuity Pathways Knowledge base to search all possible pathways that could be represented by the query proteins. The significance of each pathway was evaluated by the right-tailed Fisher's Exact test, which measures how likely it is the query proteins are relevant to the pathway. For the kinase

[5] The abbreviations used are: ROCK, Rho-associated kinase; LPA, lysophosphatidic acid; FAK, focal adhesion kinase; Crk, C-CrkII; CAS, p130crk-associated substrate; Abl, Abelson tyrosine kinase; LASP-1, lim actin-associated protein 1; Crmp-1, collapse response mediator protein 1; MAP, microtubule-associated protein; MLC, myosin light chain; CA, catalytically active; ECM, extracellular matrix.

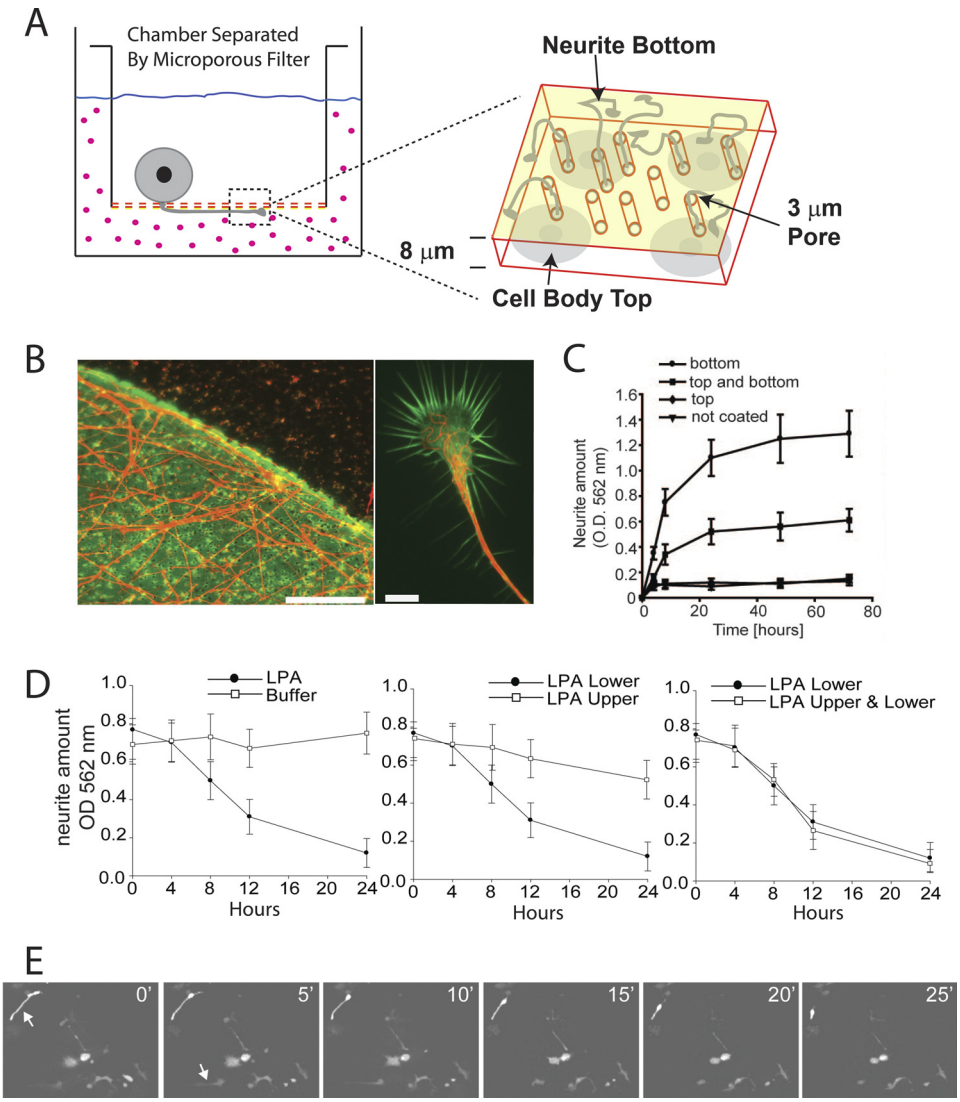

FIGURE 1. **Characterization of neurite growth and retraction kinetics using 3.0-μm porous filters and the collapsing factor LPA.** *A*, shown is a schematic of a neurite purification chamber showing neurite extension toward the lower surface of the filter coated with laminin. *B*, *left panel*, a fluorescence photomicrograph of the lower surface of the membrane shows neurites stained with α-tubulin (*red*) extending through 3.0-μm pores toward a drop of laminin (*green*) for 18 h. Note that neurites do not extend to the lower surface in the absence of laminin coating. *Right panel*, shown is a fluorescence photomicrograph of a NIE-115 neurite growth cone stained with FITC-phalloidin to visualize F-actin (*green*) and antibodies to tubulin to visualize microtubules (*red*). *Bar*, *left panel*, 30 μm; *right panel*, 10 μm. *C*, shown is quantification of neurite extension kinetics to the lower surface of 3.0-μm membranes coated with laminin on the bottom only, top only, bottom and top, or not coated with laminin. Neurites were stained with crystal violet; the dye was eluted and quantified using a spectrophotometer as described under "Experimental Procedures." S.D. from three independent experiments are shown. *D*, shown is quantification of neurite retraction kinetics in response to LPA added to the lower chamber (*left graph*), upper or lower chamber (*middle graph*), or upper and lower chamber (*right graph*) for the indicated times. *E*, shown is a fluorescence photomicrograph of a time series of neurite retraction on the lower membrane surface in response to LPA added to the lower chamber for the indicated times. The *arrow* shows retracting neurites. *Bar* = 20 μm.

phosphorylation substrate relationship analysis, we used NetworkIN software to assign possible kinases to each identified site (25). The data used for the analysis were pre-formatted using an in-house software to meet the format requirement of NetworkIN.

RESULTS

Model System for Purification of Growing and Retracting Neurites—Our previous work has shown that extending neurites can be purified from the cell body of NIE-115 cells using culture chambers equipped with 3.0-μm microporous filters (Fig. 1*A*) (35). We utilized these NIE-115 cells because they can be grown in large numbers for large-scale biochemical analysis and have been well characterized for their neuron-like properties. Laminin was coated on the bottom of the filter, which serves as a potent and directional cue for neurite initiation (35, 40–42). Neurite extension through the pore to the lower surface of the filter is β1-integrin-dependent and occurs in a highly directional and polarized manner (35). Therefore, because the cell body remains on the surface of the filter and neurite growth occurs exclusively through the pore to the lower surface, it is possible to selectively purify this structure from the polarized neuron for spatial proteomic analysis. Neurite growth under these conditions is linear for up to 24 h, reaching a maximum around 36–48 h after plating (Fig. 1, *A*–*C*). The optimal time to harvest extending neurites for biochemical analyses was 18–20

h post-plating on the laminin-coated filters. At this time the majority of neurites are elongating, have well defined growth cones, and provide sufficient amount of neurite protein for MS analysis. To obtain retracting neurites, we added the collapsing factor, LPA, to the lower chamber containing neurites that had been allowed to extend to the lower surface for 18 h (43–45). The kinetics of retraction was shown in Fig. 1*D*. Retracting neurites were harvested 10–15 min after LPA stimulation because the majority of neurites were in the process of retraction and sufficient amounts of neurite protein can still be obtained from the filter at this time. It is notable that applying LPA selectively to the cell bodies on the upper chamber surface did not significantly induce neurite retraction. These findings indicate that the neurite and soma compartments of polarized neurons are spatially sensitive to this collapsing agent through an unknown mechanism. The spatial sensitivity to guidance cues like LPA is indicative of highly polarized neurons (5–7, 17, 46–51). Also, the neurite purification system is amenable to other cells and ECM proteins including pheochromocytoma PC12 cells on fibronectin and laminin (35). These findings together with our previous work indicate that the microporous system provides a robust method to selectively purify growing or retracting neurites.

Comparison of the Neurite Phosphoproteomes from Growing and Retracting Neurites—The ability to selectively purify growing or retracting neurites independent of the soma provided a unique opportunity to study the phosphorylation/dephosphorylation mechanisms and kinase networks governing neuritogenesis in a highly spatial manner. To quantify relative changes in specific phosphorylation sites in purified growing and retracting neurites, we used immobilized metal-ion affinity chromatography to capture phosphopeptides and a liquid chromatography-mass spectrometry platform to identify parent proteins and their sites of phosphorylation as described under "Experimental Procedures" (52–56). In total, 3512 phosphopeptides were identified by MS/MS from growing and retracting neurites, representing 1883 phosphoproteins and 4145 non-redundant phosphorylation sites (supplemental Table 1). Of these peptides, 2676 were singly phosphorylated, and 836 were doubly or multiply phosphorylated. The protein identifications and sites of phosphorylation were confidently assigned with an false discovery rate of 1%.

A change in a specific phosphorylation site(s) within a phosphopeptide was considered significant with a total spectral count of 2 or more and if it either increased or decreased by at least 1.5-fold or was uniquely identified in the growing or retracting neurite fraction. All other phosphorylation sites were considered equally abundant with no specific change in both conditions. Before evaluating the relative abundance of a specific phosphopeptide in growing or retracting neurites, we first filtered the phosphopeptide dataset to remove redundancy because some peptides from the same protein may contain exactly the same phosphorylation sites due to miscleavage during tryptic digestion. After removing the redundancy, we obtained a total of 3203 phosphopeptides with unique phosphorylation status, *i.e.* even two peptides with the same amino acid sequences from the same protein must have different phosphorylation sites. The growth to retraction ratios of all

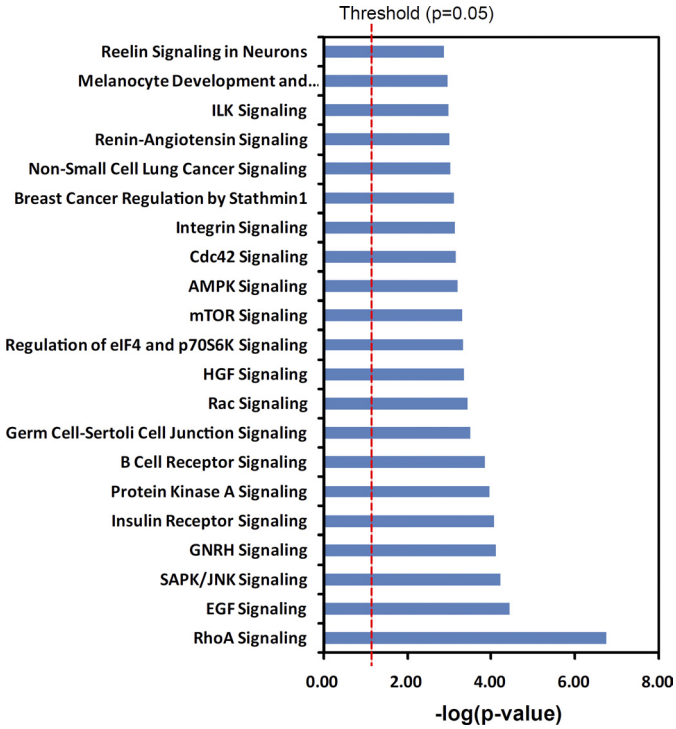

FIGURE 2. **Canonical pathways that are significantly represented by the identified phosphoproteins.** 1775 of 1883 identified phosphoproteins were mapped to the Ingenuity Pathways Analysis data base and used for pathway analysis. 78 pathways have a *p* value lower than 0.05 as determined by Fisher's test. Shown are 28 of the most significant pathways. *ILK*, Integrin linked kinase; *PAK*, p21-activated kinase; *AMPK*, AMP-activated protein kinase; *HGF*, hepatocyte growth factor; *GnRH*, gonadotropin-releasing hormone.

phosphorylation sites are shown in supplemental Table 1. Using these criteria, 513 phosphopeptides were increased in growing neurites, 368 phosphopeptides were increased in retracting neurites, and 543 phosphopeptides were equally abundant. In total, 531 proteins were observed to have altered phosphorylation sites (>1.5 or <0.67) in response to neurite extension and retraction.

Functional Annotation of Phosphoproteins Involved in Neurite Growth and Retraction—To find the functional interrelationship and assign the identified phosphoproteins that change during growth and retraction to their signaling pathways, we used the Ingenuity Pathways Analysis program and the Ingenuity Pathways Knowledge base. Ingenuity Pathways Analysis is a system-wide data base of biological pathways created from multiple relationships of proteins, genes, and diseases. The Ingenuity Pathways Analysis program can analyze large genomic or proteomic datasets to find the most statistically significant canonical pathways and protein networks relevant to the dataset based on the calculated probability score by searching the Ingenuity Pathways Knowledge base. Of a total of 78 pathways identified, RhoA signaling was the most highly represented during the growth and retraction of the neurite (Fig. 2, supplemental Fig. 1). This was expected, as RhoA signaling has been shown to play a prominent role in mediating neurite retraction in response to various collapsing factors including LPA (17, 44, 45, 57–59). Also, given that the cytoskeletal remodeling is a key event during neurite growth and retraction, it is not surprising that many pathways that regulate the

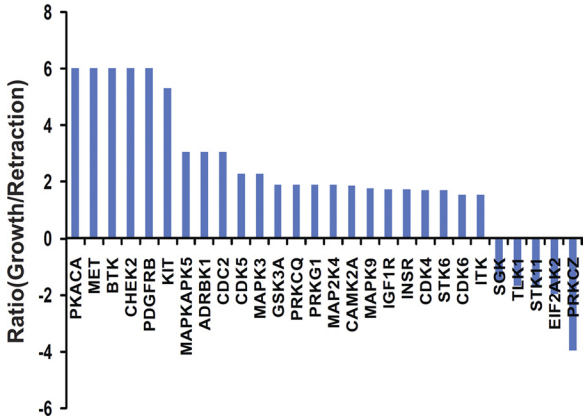

FIGURE 3. **NetworKIN annotation of kinase substrates in growing and retracting neurites.** The identified phosphosites in growing and retracting neurites were assigned to their cognate kinase class using the NetworkIN software program. The normalized ratio of the number of substrates for each kinase was calculated, and only those that have more than two substrates and with the ratio >1.5 or <0.67 were shown for comparison. *PKACA*, cAMP-dependent protein kinase catalytic subunit α; *MET*, hepatocyte growth factor receptor MET; *BTK*, Bruton tyrosine kinase; *KIT*, KIT kinase; *INSR*, insulin receptor; *ITK*, ITK tyrosine kinase; *SGK*, serine/threonine-protein kinase Sgk.

cytoskeleton were highly represented including the small GTPases Rac, RhoA, and Cdc42 as well as integrin signaling integrin linked kinase (ILK), and FAK (1, 7, 8, 17, 35, 46, 47, 60–66). Furthermore, it is notable that ERK, PI3K, and PKA kinase signaling are highly represented as these pathways are known to control cytoskeleton remodeling (66–74). Interestingly, in our previous work we reported that integrin and cytoskeleton-associated proteins were also the most abundant proteins represented in the neurite compared with the soma compartment (35). Thus, cytoskeletal proteins are highly enriched in the neurite and are the major targets modified by phosphorylation during neurite growth and retraction. Together these findings highlight the significance of using neurite purification methodology and phosphoprotein profiling to reveal signaling pathways that control neurite growth and retraction in a highly spatial manner.

Assignment of Identified Phosphorylation Sites to Known Kinases—To determine the kinases responsible for phosphorylation of neurite proteins, we utilized NetworKIN, an integrative computational approach that greatly augments kinase motif-based approaches by using contextual information to enhance kinase-substrate assignments (25, 28). The contextual information is integrated from curated pathway databases, protein interaction assays, scaffolding, co-occurrence in abstracts, physical protein interaction assays, mRNA expression studies, subcellular localization, and genomic context. Combining the contextual information with existing matrices that identify kinase domain recognition motifs has been shown to improve the accuracy of kinase-substrate assignments by 2.5-fold. Using this approach, we were able to assign specific kinases to 73.3% (737 of 1006) of the phosphorylation sites that change during neurite growth or retraction (Fig. 3). Of the 82 different kinases assigned to this process, cAMP-dependent protein kinase catalytic subunit α (PKACA), Brutons tyrosine kinase (BTK), mitogen-activated protein kinase-activated protein kinase 5 (MAPKAPK5), mitogen-activated protein kinase 3 (MAPK3 or ERK1), and PDGF receptor β kinases showed the highest ratio for the number of substrate phosphorylations in the extending neurite *versus* retracting neurites, whereas protein kinase C ζ (PRKCZ), cAMP-dependent protein kinase subunit γ (PRKACG), and lymphocyte protein tyrosine kinase (LCK) showed the lowest ratio.

ERK/MEK and RhoA Signaling Are Spatially Regulated during Neurite Growth and Retraction—Our computational analyses indicate that MEK/ERK (MAP2K4) and RhoA signaling are highly modulated in growing/retracting neurites (Figs. 2 and 3 and supplemental Fig. 1). Because the role of ERK and RhoA signaling in controlling neurite dynamics is poorly understood, we investigated these signaling pathways in more detail (40, 67, 75–81). We first directly monitored MEK and ERK kinase activities in the soma/neurite fractions using Western blotting and phosphospecific antibodies that report kinase activities of these proteins due to phosphorylation of MEK-Ser-218/Ser-222 and ERK TEY sequence (Fig. 4*A*). Both ERK and MEK kinase activities are highly increased in the extending neurite compared with the soma. The total level of ERK protein was the same in the soma and neurite compartments, whereas total MEK protein was slightly increased in the neurite. These findings demonstrate that MEK/ERK activity is highly compartmentalized to the neurite during formation of this structure. Interestingly, LPA-mediated neurite collapse induced a rapid decrease in ERK and MEK activities, which correlated with neurite retraction kinetics (Fig. 4, *A* and *B*). In contrast, Akt activity was not inhibited by LPA-induced neurite retraction (Fig. 4*C*). These findings demonstrate that in polarized neurons MEK/ERK kinase activity is highly compartmentalized within the neurite and that during neurite collapse MEK/ERK activity is shut off.

Integrins Spatially Regulate MEK Phosphorylation/Activation during Neurite Growth and Retraction—We next investigated how MEK activity and its known regulators are spatially organized in growing and retracting neurites to mediate compartmentalized ERK activity. Because we previously showed that β1 integrins drive directional neurite extension toward laminin in this model, we wanted to know if integrins played a role in MEK/ERK activation (35). During cell adhesion and membrane spreading, MEK1 activity has been shown to be regulated by integrin signals that promote phosphorylation of threonine 292 (Thr-292, human) and serine 298 (Ser-298, human) (31–34). Integrins activate the small GTPases Rac and Cdc42, which activate PAK kinase, which in turn phosphorylates MEK-Ser-298, leading to increased catalytic activity toward ERK. Interestingly, current evidence indicates that phosphorylation of MEK-Thr-292 by ERK itself negatively regulates MEK activity by decreasing PAK ability to phosphorylate MEK-Ser-298. This reduces the efficiency of MEK activity toward ERK, thereby reducing its kinase activity. In this way ERK-mediated phosphorylation of MEK-Thr-292 serves as a negative feedback loop for self-regulation. However, the role of integrin/Rac/Cdc42/PAK to MEK-Thr-292/Ser-298 phosphorylation in neurite formation has not been investigated to date.

Interestingly, in the soma we observed low levels of MEK-Ser-298 phosphorylation that was concomitant with a high level of MEK-Thr-292 phosphorylation (Fig. 4*A*). Conversely, in the extending neurite, the level of MEK-Thr-292 phosphor-

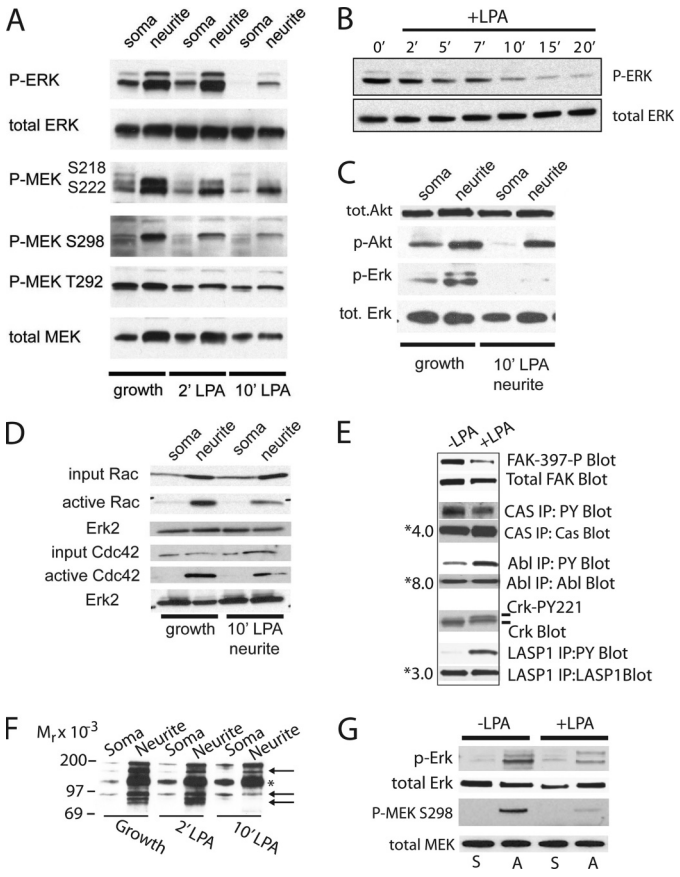

FIGURE 4. **ERK kinase activation mediates NIE-115 neurite extension.** *A*, neurons were allowed to extend neurites through 3.0-μm pores toward laminin for 12 h (growth) before LPA was added to the lower chamber for the indicated times to induce growth cone collapse and retraction. Proteins from somas or neurites were then specifically isolated as described under "Experimental Procedures" and Western-blotted with phosphosite-specific antibodies that recognize the phosphorylated activated form of ERK (*P-ERK*) or MEK (Thr-218, Thr-222, human sequence) or phosphoamino acids Ser-298 and Ser-292 of MEK, which modulate kinase activity in response to PAK and ERK kinase activity, respectively. Western blots of total cell ERK/MEK protein are shown for comparison. *B*, neurites were allowed to extend toward laminin for 18 h (time 0) then induced to collapse with LPA for the indicated times and Western-blotted for activated ERK-P and total ERK as described in A. *C*, soma and neurite proteins were prepared as in *A* and Western-blotted for the phosphorylated/activated form of Akt (p-Akt, Ser-473) or total Akt protein. *D*, cells were allowed to extend neurites for 18 h (growth) and then stimulated with LPA to induce retraction. Rac and Cdc42 activation (Rac-GTP, Cdc42-GTP) were determined from isolated neurite and soma proteins using a GST-PBD pull-down assay and Western blot analyses. ERK served as the loading control. *E*, cells were allowed to extend neurites to the lower surface for 8 h (growth) and then stimulated with LPA for the indicated times. Somas and neurites were purified and Western-blotted for the indicated proteins and/or specific phosphorylation sites. Crk Tyr-221 (*PY*) phosphorylation was detected as a decrease in electrophoretic mobility in the gel. LASP-1 was first immunoprecipitated (*IP*) and then Western-blotted with anti-phosphotyrosine antibodies. The *asterisk* indicates the neurite/soma fold enrichment of the protein as determined by mass spectrometry and or Western blotting and densitometry. *F*, cells were allowed to extend neurites to the lower surface for 8 h (growth) and then stimulated with LPA for the indicated times. Somas and neurites were purified and Western-blotted with anti-phosphotyrosine antibodies. *Arrows* show neurite-specific proteins that decrease in response to LPA. The *asterisk* shows a neurite protein band that does not change in response to LPA. *G*, N1E-115 cells were either held in suspension (*S*) or allowed to attach (*A*) to laminin-coated dishes for 45 min in the presence or absence of LPA and then Western-blotted for activated ERK (*p-ERK*) or MEK Ser-298 as in *A*.

ylation was decreased relative to the level of MEK Ser-298 phosphorylation, which is consistent with the high level of ERK activity in this compartment (Fig. 4*A*). The increased ratio of MEK Thr-292/Ser-298 phosphorylation relative to the small pool of activated ERK present in the soma indicates that MEK activity is strongly inhibited in the soma due to the negative feedback modulation by ERK. These findings are consistent with the idea that the low level of ERK activity in the soma (Fig. 4*A*) results from the uncoupling of PAK from MEK-Ser-298 phosphorylation. On the other hand, negative feedback modulation of MEK by ERK in the neurite is significantly attenuated, leading to robust MEK-Ser-298 phosphorylation and increased ERK kinase activity. Thus, in the neurite MEK/ERK activity is robust and strongly coupled to integrin/PAK signaling, whereas in the soma ERK activity is low and not uncoupled to integrin/PAK signaling due to strong negative feedback modulation by ERK. These findings suggest that integrins drive directional neurite extension through compartmentalized PAK/MEK/ERK signaling. These findings are further supported by the observation that Cdc42 and Rac activities are significantly elevated in the neurite compared with the soma (Fig. 4*D*). We also detected several PAK family members (1, 2, 4) that are present in the neurite and modified by phosphorylation (supplemental Table 1).

LPA-induced Neurite Collapse Disrupts Integrin/PAK/Rac/Cdc42/MEK/ERK Signaling—In the neurite, the level of Ser-298 phosphorylation decreased in response to LPA-induced collapse, which correlated with the loss of ERK, Cdc42, and Rac activities (Fig. 4, *A–D*). As expected, MEK-Thr-292 phosphorylation by ERK decreased in response to the loss of ERK activity (Fig. 4*A*). These findings suggest that LPA induces neurite collapse and ERK activity by interfering with integrin adhesion signaling to Rac/Cdc42/PAK and MEK-Ser-298 phosphorylation. In support of these findings, LPA blocked ERK activation and MEK Ser-298 phosphorylation induced by integrin-mediated NIE-115 cell attachment and spreading on laminin (Fig. 4*G*). In addition, LPA was found to modulate tyrosine phosphorylation of several known integrin/focal adhesion-associated proteins (FAK, CAS, Abl, Lasp-1, Crk) (Fig. 4, *E* and *F*) (82–85). It is also notable that LPA treatment decreased CAS phosphorylation, whereas it increased Crk Tyr-221 phosphorylation and Abl/Arg tyrosine phosphorylation (Fig. 4*E*). These phosphorylation events have been previously associated with decreased CAS/Crk coupling and Rac activity in spreading cells downstream of integrin receptors (83–85). Taken together these findings suggest that neurite extension involves integrin activation of the CAS/Crk/Rac/Cdc42/PAK/MEK-Ser-298/ERK signaling pathway, whereas LPA-induced collapse blocks activation of integrin signaling leading to neurite detachment and retraction from the substrate.

Integrin Regulation of MEK/ERK Activity Is Necessary for Neurite Growth and Retraction—To investigate the functional significance of MEK/ERK activity in neuritogenesis, we expressed mutationally activated MEK (MEK-S211E/S222E, catalytically active MEK, MEK-CA) in cells and then examined neurite formation toward laminin (Fig. 5, *A* and *D*). This phosphomimetic mutation promoted constitutive ERK activation and increased neurite formation (Fig. 5*A*). Interestingly, substitution of Ser-298 with an alanine residue in MEK-CA partially reduced neurite formation, suggesting that this site of phosphorylation does contribute to MEK/ERK-induced neurite for-

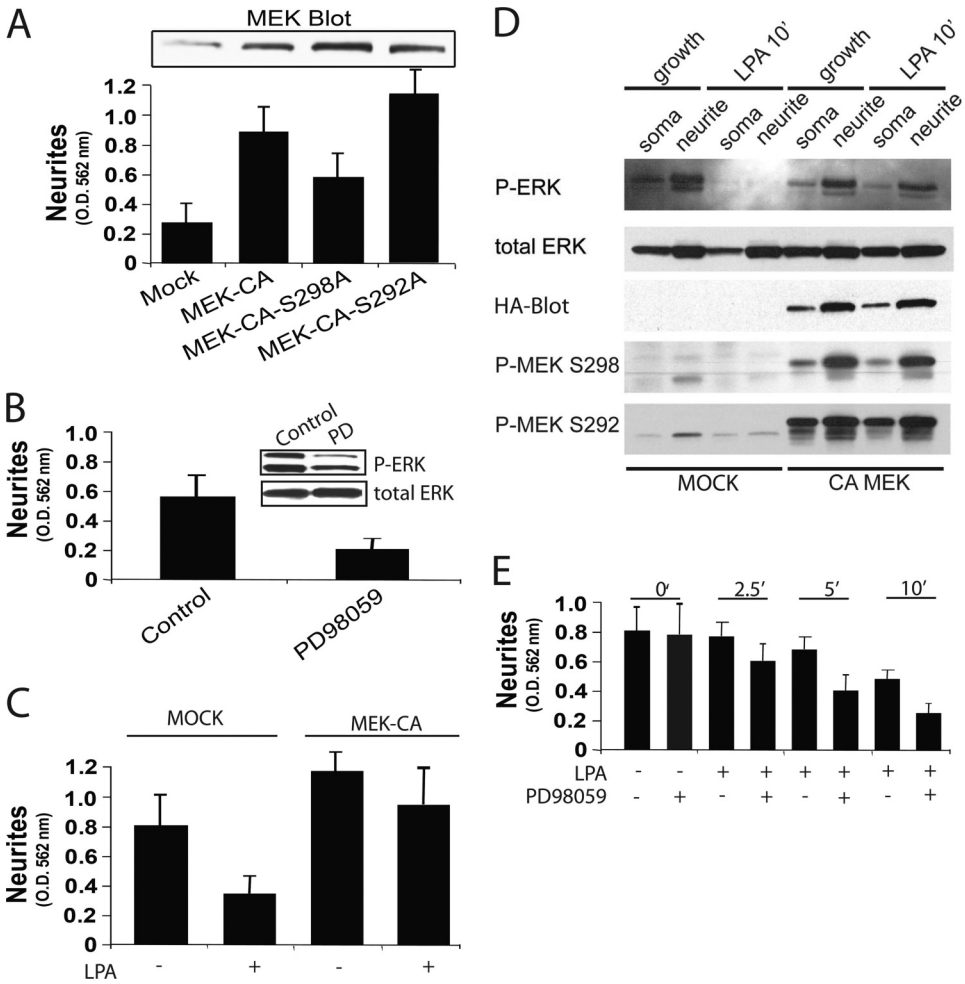

FIGURE 5. **Deactivation of ERK is necessary for LPA-induced N1E-115 neurite retraction.** *A*, quantification is shown of neurite formation of NIE-115 cells either mock-transfected or transfected with constructs encoding mutationally activated MEK (*MEK-CA*) or MEK-CA with Ser-298 or Ser-292 amino acids changed to alanine. Inset shows the level of MEK expression by Western blotting. *B*, shown is quantification of neurite formation for 6 h in the presence of the MEK kinase inhibitor PD98059 (25 μm) or the vehicle DMSO (control). The *inset* shows the level of ERK phosphorylation and kinase activity by Western blotting as described in Fig. 4*A*. *C*, cells were either mock-transfected with an empty vector or transfected with HA-tagged MEK-CA and allowed to extend neurites to the lower surface for 18 h and then treated with or without LPA for 10 min to induce retraction and quantified as described in Fig. 1*D*. *D*, somas and neurites were purified from cells transfected as in *C* and Western-blotted with phosphospecific antibodies to activated p-ERK and MEK phosphorylated on Ser-292 or Ser-298. HA-MEK and total ERK Western blots are shown for comparison. *E*, cells were allowed to extend neurites to the lower membrane surface for 12 h then treated with the MEK inhibitor PD98059 for 60 min (time 0) before being treated with or without LPA for the indicated times. Neurites were quantified as in Fig. 1*D*.

mation even when MEK is constitutively activated. In contrast, MEK-CA with Thr-292 mutated to alanine increased neurite formation probably because MEK is no longer susceptible to negative feedback regulation by ERK (Fig. 5*A*). MEK kinase activity was required for neurite formation, as treatment of cells with the MEK inhibitor PD98059 blocked ERK activation and neurite formation on laminin (Fig. 5*B*). These findings indicate that MEK activation is sufficient and necessary to induce neurite formation, and this response is partially regulated by MEK-Ser-298/Thr-292 phosphorylation.

Inhibition of MEK/ERK Activity Is Necessary for RhoA/ROCK/MLC-mediated Neurite Retraction—We next investigated whether MEK/ERK inactivation is required for neurite retraction. NIE-115 cells expressing a mutationally active form of MEK1 (MEK-CA) were treated with LPA and monitored for neurite retraction and ERK kinase inactivation. Strikingly, LPA did not induce neurite retraction or inhibit ERK activation in MEK-CA cells nor did it prevent Ser-298 phosphorylation (Fig. 5, *C* and *D*). The fact that phosphorylation of MEK-Ser-298 is not inhibited by LPA treatment in MEK-CA cells suggests that ERK activation provides a positive feedback mechanism to maintain integrin/Rac/Cdc42/PAK signaling in the neurite, thereby preventing neurite detachment and retraction from the ECM. Interestingly, although inhibition of MEK/ERK activity with PD98059 did not induce neurite retraction by itself, it did increase retraction induced by a suboptimal dose of LPA (50% of the maximum) (Fig. 5*E*). Thus, although the loss of ERK activity is not sufficient to induce neurite retraction *per se*, it does sensitize the cell to LPA-mediated retraction. These findings suggest that LPA-induced neurite retraction not only requires ERK deactivation but also involves activation/deactivation of additional signaling pathways. RhoA activation is a likely candidate as LPA-induced neurite retraction requires RhoA activation, which facilitates ROCK-mediated myosin contraction (supplemental Fig. 1) (7, 17, 57, 86–88). Consistent with these observations, the ROCK kinase inhibitor Y-27632

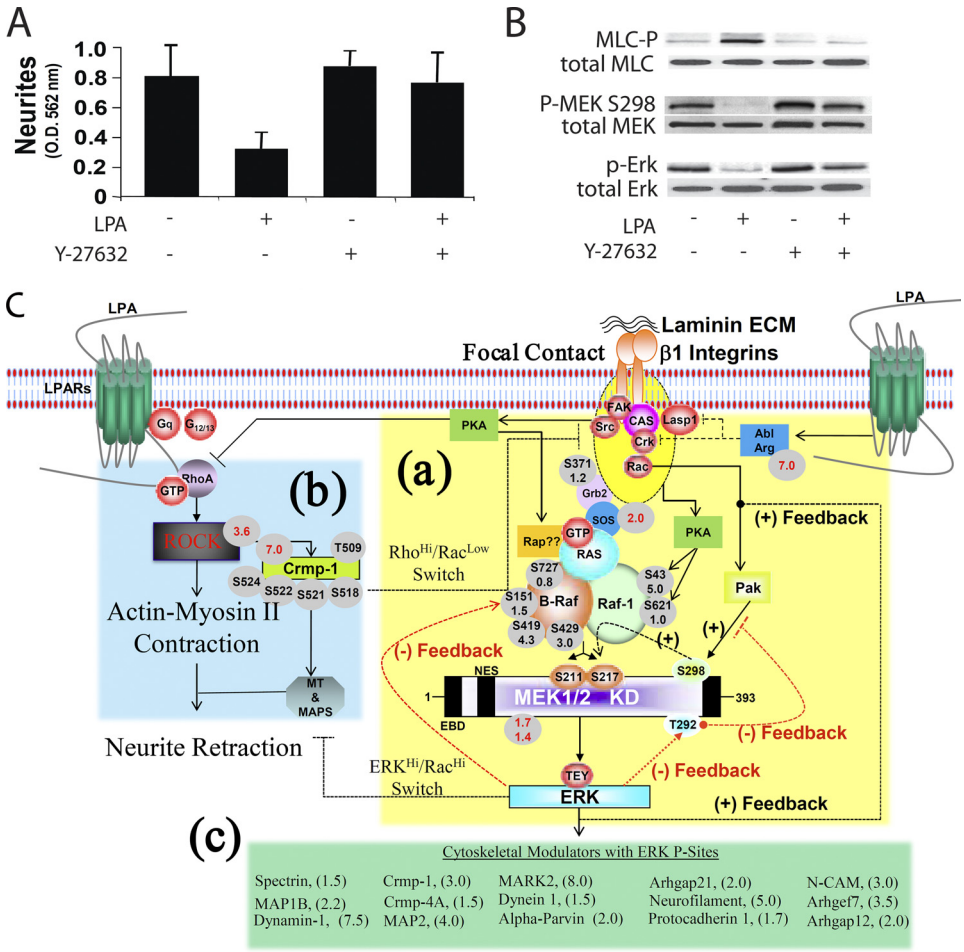

FIGURE 6. **Inhibition of ROCK kinase activity prevents LPA-induce N1E-115 neurite retraction and prevents ERK inactivation.** *A*, neurites were allowed to extend to the lower surface of the membrane for 18 h and then treated with or without the ROCK kinase inhibitor Y-27632 for 30 min before being stimulated with or without LPA for 10 min. Neurites were quantified as described in Fig. 1*D*. *B*, neurites were isolated from cells treated as in *A* and Western-blotted for activated ERK (*p-ERK*) or phosphorylated myosin light chain (*MLC-P*) on serine 19 or total MLC. *C*, a schematic model shows the possible signaling and phosphorylation mechanisms that mediate neurite extension and retraction in response to the collapsing factor LPA. *Gray-shaded circles with black text* indicate the phosphorylation site and neurite growth/retraction ratio determined by mass spectrometry. *Red text* indicates -fold change in protein abundance level between soma and neurite. A list of the depicted proteins and their associated regulatory molecules and their neurite abundance and phosphorylation status is shown in supplemental Table 3. *a* shows integrin-mediated ERK activation and the neurite extension pathway. *b* shows LPA the induced neurite retraction pathway. Also see supplemental Fig. 1 for more details of the LPA/Rho pathway. *c* shows cytoskeleton-associated proteins that contain at least one phosphorylation site that conforms to the ERK amino acid consensus sequence P*X*(S)TP where *X* is any basic or neutral amino acid. *Numbers in parentheses* indicate the neurite growth/retraction ratio of the predicated ERK phosphorylation site as measured by mass spectrometry. *MT*, microtubules, MAPS, microtubule-associated proteins; LPAR, LPA receptor. *PRKCZ*, Protein kinase C ζ; *PRKACG*, cAMP-dependent protein kinase subunit γ; *LCK*, lymphocyte protein tyrosine kinase; *NES*, Nuclear Exclusion sequence; *EBD*, ERK binding domain and *KD*, Kinase Domain.

prevented neurite retraction and myosin contraction as indicated by a decrease in serine 19 phosphorylation of myosin light chain (Fig. 6, *A* and *B*) (7, 88). Importantly, Y-27632 not only prevented neurite retraction but also blocked LPA-induced ERK deactivation and MEK-Ser-298 phosphorylation in the neurite fraction (Fig. 6*B*). Thus, inhibition of integrin/Rac-Cdc42/PAK/MEK/ERK signaling is necessary for LPA-RhoA/ROCK/MLC-mediated neurite retraction. Based on our functional proteomics work and the work of others we proposed a model for how neurites extend and retract in response to laminin and LPA. The model is shown schematically in Fig. 6*C* and supplemental Fig. 1 and is discussed below.

DISCUSSION

Our ability to differentially isolate neurites in a state of growth or retraction for proteomic analyses provided a simple and robust system to globally profile thousands of protein phosphorylation and kinase changes that mediate neuritogenesis. An important aspect of this model system is the ability to specifically isolate the neurite from the soma for proteomic analyses. This unique strategy allowed us to mine deeper into the neurite phosphoproteome, uncovering many more low abundant phosphoproteins. Because of this, we were able to obtain a more precise picture of the complex spatial kinase/substrate networks that control neurite growth/retraction kinetics. Also, the neurite purification methods described here will likely transfer to other neuronal cell types, guidance factors, and collapsing agents. For example, we have previously reported that neurites can be readily purified from PC12 cells responding to laminin and fibronectin guidance cues (35). It may also be possible to selectively purify axons and dendrites from primary neurons for detailed proteomic analyses using specific differentiation and/or guidance factors. In any case, the utility of this model system combined with the rapid progress being made in

quantitative mass spectrometry will help provide a more comprehensive understanding of the neurite proteome and its spatial organization, which in turn will provide valuable insight into the various disease pathologies caused by deregulation of this process.

Using NetworKIN, we find that a large panel of kinases is active during neurite growth, whereas a relatively reduced number of kinases are active during retraction. Many of these kinases have been previously implicated in the regulation of different aspects of neurite outgrowth. PKA (PKACA) can trigger neurite outgrowth by phosphorylating synapsins (89) and CREB (cAMP-response element-binding protein) (90). The MET receptor (MET) enhances axonal outgrowth of cultured dorsal root ganglions by potentiating NGF signaling (91). The tyrosine kinase BTK (*BTK*) phosphorylates the actin regulator N-WASP, which is essential for neurite outgrowth (92). The cyclin kinase Cdk5 (CDK5) regulates neurite and axon outgrowth by phosphorylating the kinase PAK1 and the microtubule-associated protein MAP1B (93). GSK3 (*GSK3A*) phosphorylates the collapsin response mediator protein-2 (Crmp-2) to promote neurite elongation via microtubule assembly (94). The MAP kinase kinase MKK4 (MAP2K4) and its substrate JNK (MAPK9) have also been involved in the regulation of neurite outgrowth through the phosphorylation of the microtubule binding proteins MAP, MAP1, doublecortin, and SGC10 (95). Although these findings point to a wide array of kinase classes that regulate neuritogenesis, it is likely that they work together in time and space to fine-tune changes in the actin and microtubule cytoskeletons that drive this process. Using similar proteomics and bioinformatic methods, we recently revealed a Rho GTPase signaling network that regulates neurite outgrowth (35). This allowed us to uncover an unexpected signaling complexity, with different Rho GTPase signaling modules operating in time and space to regulate distinct neurite functions including neurite initiation, elongation, pathfinding, and filopodial stabilization. Similarly, the wide kinase activation and signal annotation profiles we observes hint to a high degree of modularity in fine tuning neuritogenesis. On the other hand, the precise functions of the protein kinases that modulate LPA-induced neurite collapse were less clear from our phosphoproteomic datasets. However, one of these kinases, serum- and glucocorticoid-inducible kinase 1, regulates microtubule depolymerization and the shortening of neuronal processes (96). It will be important in the future to systematically probe these different kinase-substrate networks to reveal their specialized contribution to the dynamic processes of neurite growth and retraction.

Our combined informatics and functional studies revealed that integrin to MEK/ERK signaling plays a prominent role in controlling neuritogenesis. Based on our findings and the work of others, we have constructed a working model for how MEK/ERK activation and deactivation by LPA control neuritogenesis (Fig. 6*C*). The signaling components that were used to construct the schematic and their relative abundance in the soma and neurite as well as their observed phosphorylation sites are listed in Fig. 6*C* and supplemental Table 3. Fig. 6C *panel a* shows the proposed pathway for how integrins mediate ERK activation leading to neurite extension. ECM proteins like laminin and fibronectin are present as adhesive gradients in the extracellular environment that can initiate and guide neurite protrusion from the cell body through activation of integrin receptors and the recruitment of their downstream effectors including FAK/CAS/Crk (8, 83, 84). This canonical pathway operates spatially in the neurite to drive localized Rac activation of PAK. PAK then phosphorylates MEK Ser-298, leading to enhanced MEK and ERK activity as described in non-neuronal cells (31–34). The integrin/Rac/PAK/MEK-Ser-298 signaling cascade promotes strong sustained ERK activation, which serves as a switch to mediate neurite outgrowth while suppressing basal RhoA/ROCK/MLC-mediated membrane contractility, possibly through PKA activation (*panel b*).

Although the spatial mechanisms that promote localized ERK activation in the neurite are not clear, the integrin/Rac/PAK activation pathway most likely works in close conjunction with common upstream activators of MEK including Rap-1, Ras, and Raf (22, 97–102). These upstream signals fully activate MEK through phosphorylation of Ser-218/Ser-222 (103, 104). It is notable that although MEK activation may occur through either B-Raf and/or Raf-1 activation, our phosphoproteomics work suggests that B-Raf is more likely involved as Raf-1 is highly phosphorylated on Ser-43 (growth specific) in extending neurites (supplemental Table 1). Ser-43 phosphorylation has previously been associated with PKA activation and is inhibitory to Raf-1 kinase activity (105, 106). How then is B-Raf activity modulated to increase MEK/ERK signaling? Integrin activation of Rap-1 can modulate B-Raf activity, as can cAMP/PKA signaling (102). Rap1A and -B isoforms are present in the neurite, and several Rap1 GEF (guanine nucleotide exchange factor) and GAP (GTPase-activating protein) effector proteins are differentially phosphorylated during neurite growth and retraction (supplemental Table 1). Rap activity and its effectors could be modulated directly or indirectly by integrin activation and/or cell spreading on laminin, possibly through PKA activation (102). Alternatively, integrin activation of FAK/Src can facilitate activation of the canonical Grb2 (growth factor rector-bound protein 2)/SOS (son of sevenless)/Ras/Raf/MEK/ERK pathway (22). In the end, ERK activity self-regulates by modulation of its upstream activators through negative feedback phosphorylation of MEK-S292, which suppresses PAK phosphorylation of 298 and phosphorylation of B-Raf-Ser-151, which inhibits B-Raf activity (102). Fig. 6*C panel c* shows a list of cytoskeletal effector proteins that are either known and/or predicted to be phosphorylated by ERK and, thus, may modulate neurite growth. Of particular interest are α-parvin, which modulates focal adhesion and actin cytoskeletal dynamics and the microtubule modulating proteins Crmp-1, MARK2 (microtubule-associated regulatory kinase 2), MAP1B, and MAP2 (10, 107–109). Supplemental Table 2 shows a complete list of all identified phosphoproteins with ERK consensus phosphorylation signatures.

An important finding in our study was that LPA could disrupt integrin signaling, leading to blockade of the CAS/Crk/Rac/PAK/MEK/ERK pathway (Fig. 6C, *panels a* and *b*). We suspect that this facilitates neurite detachment from the ECM by losing integrin adhesions to the substratum while activating the Rho/ROCK contractile mechanisms that physically mediate

growth cone collapse and membrane retraction through force generation (Fig. 6*C* and supplemental Fig. 1) (7). Interestingly, the RhoA/ROCK/MLC pathway has been reported to mediate neurite collapse by modulating Crmp family proteins and microtubule dynamics (5, 108–110). In our work here, Crmp-1 was observed to be enriched by 7-fold in the neurite and to be differentially phosphorylated on multiple sites in neurites undergoing growth or retraction (supplemental Table 1). Although the mechanisms that block LPA-induced integrin signaling in the neurite are not defined, Abl family kinases (Abl and Arg) are likely to play a central role through their ability to modulate CAS/Crk coupling and Rac activity at adhesion sites as described (8, 83–85, 111–113). Importantly, we found that Abl is hypertyrosine-phosphorylated and enriched by 7-fold in the neurite. Also, Abl itself and its known substrates c-CrkII Tyr-221 and LASP-1 show increased phosphorylation in the neurite in response to LPA (Fig. 4*E*) (82). This suggests that LPA activates Abl kinase, which in turn tyrosine phosphorylates Crk at Tyr-221, inhibiting CAS/Crk coupling and downstream Rac/PAK/MEK activation. It is also notable that LPA did not inhibit MEK-Ser-298 phosphorylation by PAK in cells expressing constitutively activated MEK, which was associated with decreased neurite retraction (Fig. 5, *A* and *D*). This suggests that MEK/ERK signaling provides a positive feedback to maintain integrin/CAS/Crk/Rac/PAK signaling and, thus, prevents neurite retraction.

Taken together our work and the work of others suggest a model whereby the net effect of high Rac/PAK/MEK/ERK activation and RhoA inhibition is increased membrane protrusion and decreased neurite contraction events leading to net neurite growth. Increased Rac activity has been shown to suppress RhoA signaling, which leads to neurite growth in neurons (7, 114). PKA and ERK signaling can also suppress RhoA signaling in other cell types (115–117). On the other hand, LPA strongly activates RhoA/ROCK/MLC and Abl kinase, which together mediate neurite detachment from the ECM and membrane contraction, leading to growth cone turning and/or collapse. In this model Rac/PAK/MEK/ERK signaling serves as a spatially compartmentalized switch that operates downstream of integrin and LPA receptor activation to modulate neurite growth and retraction kinetics, respectively. Our findings provide a plausible mechanism for how neuronal growth cones spatially interpret extracellular cues and navigate through complex tissues, which is critical for proper brain development and spinal cord regeneration.

Acknowledgments—We thank Monica Holcomb for excellent technical assistance. We also thank Dr. Andrew D. Catling (Louisiana State University Health Sciences Center, New Orleans, LA) for providing the MEK constructs and Drs. Rune Linding and Tony Pawson for assistance and advice on using NetworKIN. Portions of the research were performed in the Environmental Molecular Sciences Laboratory, a United States Department of Energy scientific user facility located at Pacific Northwest National Laboratory in Richland, WA. Pacific Northwest National Laboratory is operated by Battelle for the United States Department of Energy under Contract DE-AC05-76RLO 1830.

REFERENCES

1. Giannone, G., Mège, R. M., and Thoumine, O. (2009) *Trends Cell Biol.* **19,** 475–486
2. Drees, F., and Gertler, F. B. (2008) *Curr. Opin. Neurobiol.* **18,** 53–59
3. Koh, C. G. (2006) *Neurosignals* **15,** 228–237
4. Allen, J., and Chilton, J. K. (2009) *Dev. Biol.* **327,** 4–11
5. Arimura, N., and Kaibuchi, K. (2005) *Neuron* **48,** 881–884
6. Fukata, M., Nakagawa, M., and Kaibuchi, K. (2003) *Curr. Opin. Cell Biol.* **15,** 590–597
7. Nikolic, M. (2002) *Int. J. Biochem. Cell Biol.* **34,** 731–745
8. Dent, E. W., and Gertler, F. B. (2003) *Neuron* **40,** 209–227
9. Jeon, S., Park, J. K., Bae, C. D., and Park, J. (2010) *Neurochem. Int.* **56,** 810–818
10. Dehmelt, L., and Halpain, S. (2007) *Curr. Biol.* **17,** R611–R614
11. Yamauchi, J., Miyamoto, Y., Sanbe, A., and Tanoue, A. (2006) *Exp. Cell Res.* **312,** 2954–2961
12. Nusser, N., Gosmanova, E., Makarova, N., Fujiwara, Y., Yang, L., Guo, F., Luo, Y., Zheng, Y., and Tigyi, G. (2006) *Cell. Signal.* **18,** 704–714
13. Jørgensen, C., Sherman, A., Chen, G. I., Pasculescu, A., Poliakov, A., Hsiung, M., Larsen, B., Wilkinson, D. G., Linding, R., and Pawson, T. (2009) *Science* **326,** 1502–1509
14. Round, J., and Stein, E. (2007) *Curr. Opin. Neurobiol.* **17,** 15–21
15. Woodring, P. J., Litwack, E. D., O'Leary, D. D., Lucero, G. R., Wang, J. Y., and Hunter, T. (2002) *J. Cell Biol.* **156,** 879–892
16. Spencer, T. K., Mellado, W., and Filbin, M. T. (2008) *Mol. Cell. Neurosci.* **38,** 110–116
17. Hirose, M., Ishizaki, T., Watanabe, N., Uehata, M., Kranenburg, O., Moolenaar, W. H., Matsumura, F., Maekawa, M., Bito, H., and Narumiya, S. (1998) *J. Cell Biol.* **141,** 1625–1636
18. Manning, G., Whyte, D. B., Martinez, R., Hunter, T., and Sudarsanam, S. (2002) *Science* **298,** 1912–1934
19. Alonso, A., Sasin, J., Bottini, N., Friedberg, I., Friedberg, I., Osterman, A., Godzik, A., Hunter, T., Dixon, J., and Mustelin, T. (2004) *Cell* **117,** 699–711
20. Manning, G., Plowman, G. D., Hunter, T., and Sudarsanam, S. (2002) *Trends Biochem. Sci.* **27,** 514–520
21. Kim, E. K., and Choi, E. J. (2010) *Biochim. Biophys. Acta* **1802,** 396–405
22. Yee, K. L., Weaver, V. M., and Hammer, D. A. (2008) *IET Syst. Biol.* **2,** 8–15
23. Ramos, J. W. (2008) *Int. J. Biochem. Cell Biol.* **40,** 2707–2719
24. Pullikuth, A. K., and Catling, A. D. (2007) *Cell. Signal.* **19,** 1621–1632
25. Linding, R., Jensen, L. J., Ostheimer, G. J., van Vugt, M. A., Jørgensen, C., Miron, I. M., Diella, F., Colwill, K., Taylor, L., Elder, K., Metalnikov, P., Nguyen, V., Pasculescu, A., Jin, J., Park, J. G., Samson, L. D., Woodgett, J. R., Russell, R. B., Bork, P., Yaffe, M. B., and Pawson, T. (2007) *Cell* **129,** 1415–1426
26. Jørgensen, C., and Linding, R. (2010) *Curr. Opin. Genet. Dev.* **20,** 15–22
27. Tan, C. S., and Linding, R. (2009) *Proteomics* **9,** 5233–5242
28. Linding, R., Jensen, L. J., Pasculescu, A., Olhovsky, M., Colwill, K., Bork, P., Yaffe, M. B., and Pawson, T. (2008) *Nucleic Acids Res.* **36,** D695–D699
29. Van Hoof, D., Muñoz, J., Braam, S. R., Pinkse, M. W., Linding, R., Heck, A. J., Mummery, C. L., and Krijgsveld, J. (2009) *Cell Stem Cell* **5,** 214–226
30. van Vugt, M. A., Gardino, A. K., Linding, R., Ostheimer, G. J., Reinhardt, H. C., Ong, S. E., Tan, C. S., Miao, H., Keezer, S. M., Li, J., Pawson, T., Lewis, T. A., Carr, S. A., Smerdon, S. J., Brummelkamp, T. R., and Yaffe, M. B. (2010) *PLoS Biol* **8,** e1000287
31. Park, E. R., Eblen, S. T., and Catling, A. D. (2007) *Cell. Signal.* **19,** 1488–1496
32. Eblen, S. T., Slack-Davis, J. K., Tarcsafalvi, A., Parsons, J. T., Weber, M. J., and Catling, A. D. (2004) *Mol. Cell. Biol.* **24,** 2308–2317
33. Slack-Davis, J. K., Eblen, S. T., Zecevic, M., Boerner, S. A., Tarcsafalvi, A., Diaz, H. B., Marshall, M. S., Weber, M. J., Parsons, J. T., and Catling, A. D. (2003) *J. Cell Biol.* **162,** 281–291
34. Eblen, S. T., Slack, J. K., Weber, M. J., and Catling, A. D. (2002) *Mol. Cell. Biol.* **22,** 6023–6033
35. Pertz, O. C., Wang, Y., Yang, F., Wang, W., Gay, L. J., Gristenko, M. A., Clauss, T. R., Anderson, D. J., Liu, T., Auberry, K. J., Camp, D. G., 2nd,

Smith, R. D., and Klemke, R. L. (2008) *Proc. Natl. Acad. Sci. U.S.A.* **105,** 1931–1936
36. Yang, F., Waters, K. M., Miller, J. H., Gritsenko, M. A., Zhao, R., Du, X., Livesay, E. A., Purvine, S. O., Monroe, M. E., Wang, Y., Camp, D. G., 2nd, Smith, R. D., and Stenoien, D. L. (2010) *PLoS One* **5,** e14152
37. Du, X., Yang, F., Manes, N. P., Stenoien, D. L., Monroe, M. E., Adkins, J. N., States, D. J., Purvine, S. O., Camp, D. G., 2nd, and Smith, R. D. (2008) *J. Proteome Res.* **7,** 2195–2203
38. Beausoleil, S. A., Villén, J., Gerber, S. A., Rush, J., and Gygi, S. P. (2006) *Nat. Biotechnol.* **24,** 1285–1292
39. Heibeck, T. H., Ding, S. J., Opresko, L. K., Zhao, R., Schepmoes, A. A., Yang, F., Tolmachev, A. V., Monroe, M. E., Camp, D. G., 2nd, Smith, R. D., Wiley, H. S., and Qian, W. J. (2009) *J. Proteome Res.* **8,** 3852–3861
40. Mruthyunjaya, S., Manchanda, R., Godbole, R., Pujari, R., Shiras, A., and Shastry, P. (2010) *Biochem. Biophys. Res. Commun.* **391,** 43–48
41. Plantman, S., Patarroyo, M., Fried, K., Domogatskaya, A., Tryggvason, K., Hammarberg, H., and Cullheim, S. (2008) *Mol. Cell. Neurosci.* **39,** 50–62
42. Li, G. N., Liu, J., and Hoffman-Kim, D. (2008) *Ann. Biomed. Eng.* **36,** 889–904
43. Sayas, C. L., Moreno-Flores, M. T., Avila, J., and Wandosell, F. (1999) *J. Biol. Chem.* **274,** 37046–37052
44. Kranenburg, O., Poland, M., van Horck, F. P., Drechsel, D., Hall, A., and Moolenaar, W. H. (1999) *Mol. Biol. Cell* **10,** 1851–1857
45. Tigyi, G., Fischer, D. J., Sebök, A., Yang, C., Dyer, D. L., and Miledi, R. (1996) *J. Neurochem.* **66,** 537–548
46. O'Donnell, M., Chance, R. K., and Bashaw, G. J. (2009) *Annu. Rev. Neurosci.* **32,** 383–412
47. Lowery, L. A., and Van Vactor, D. (2009) *Nat. Rev. Mol. Cell Biol.* **10,** 332–343
48. Xiang, Y., Li, Y., Zhang, Z., Cui, K., Wang, S., Yuan, X. B., Wu, C. P., Poo, M. M., and Duan, S. (2002) *Nat. Neurosci.* **5,** 843–848
49. Dickson, B. J. (2001) *Curr. Opin. Neurobiol.* **11,** 103–110
50. Kalil, K., Szebenyi, G., and Dent, E. W. (2000) *J. Neurobiol.* **44,** 145–158
51. van Horck, F. P., Weinl, C., and Holt, C. E. (2004) *Curr. Opin. Neurobiol.* **14,** 61–66
52. Liang, X., Fonnum, G., Hajivandi, M., Stene, T., Kjus, N. H., Ragnhildstveit, E., Amshey, J. W., Predki, P., and Pope, R. M. (2007) *J. Am. Soc. Mass Spectrom.* **18,** 1932–1944
53. Moser, K., and White, F. M. (2006) *J. Proteome Res.* **5,** 98–104
54. Brill, L. M., Salomon, A. R., Ficarro, S. B., Mukherji, M., Stettler-Gill, M., and Peters, E. C. (2004) *Anal. Chem.* **76,** 2763–2772
55. Ding, S. J., Wang, Y., Jacobs, J. M., Qian, W. J., Yang, F., Tolmachev, A. V., Du, X., Wang, W., Moore, R. J., Monroe, M. E., Purvine, S. O., Waters, K., Heibeck, T. H., Adkins, J. N., Camp, D. G., 2nd, Klemke, R. L., and Smith, R. D. (2008) *J. Proteome Res.* **7,** 4215–4224
56. Wang, Y., Ding, S. J., Wang, W., Jacobs, J. M., Qian, W. J., Moore, R. J., Yang, F., Camp, D. G., 2nd, Smith, R. D., and Klemke, R. L. (2007) *Proc. Natl. Acad. Sci. U.S.A.* **104,** 8328–8333
57. To, K. C., Church, J., and O'Connor, T. P. (2008) *Neuroscience* **153,** 645–653
58. Sayas, C. L., Avila, J., and Wandosell, F. (2002) *Biochim. Biophys. Acta* **1582,** 144–153
59. Fukushima, N., Weiner, J. A., Kaushal, D., Contos, J. J., Rehen, S. K., Kingsbury, M. A., Kim, K. Y., and Chun, J. (2002) *Mol. Cell. Neurosci.* **20,** 271–282
60. Tucker, B. A., Rahimtula, M., and Mearow, K. M. (2008) *Cell. Signal.* **20,** 241–257
61. Ivankovic-Dikic, I., Grönroos, E., Blaukat, A., Barth, B. U., and Dikic, I. (2000) *Nat. Cell Biol.* **2,** 574–581
62. Vogelezang, M., Forster, U. B., Han, J., Ginsberg, M. H., and ffrench-Constant, C. (2007) *BMC Neurosci.* **8,** 44
63. Tahirovic, S., Hellal, F., Neukirchen, D., Hindges, R., Garvalov, B. K., Flynn, K. C., Stradal, T. E., Chrostek-Grashoff, A., Brakebusch, C., and Bradke, F. (2010) *J. Neurosci.* **30,** 6930–6943
64. Prager-Khoutorsky, M., and Spira, M. E. (2009) *Brain Res.* **1251,** 65–79
65. Geraldo, S., and Gordon-Weeks, P. R. (2009) *J. Cell Sci.* **122,** 3595–3604
66. Quinn, C. C., and Wadsworth, W. G. (2008) *Trends Cell Biol.* **18,** 597–603
67. Yasui, H., Ito, N., Yamamori, T., Nakamura, H., Okano, J., Asanuma, T., Nakajima, T., Kuwabara, M., and Inanami, O. (2010) *Free Radic. Res.* **44,** 645–654
68. Shelly, M., Lim, B. K., Cancedda, L., Heilshorn, S. C., Gao, H., and Poo, M. M. (2010) *Science* **327,** 547–552
69. Wu, H., Ichikawa, S., Tani, C., Zhu, B., Tada, M., Shimoishi, Y., Murata, Y., and Nakamura, Y. (2009) *Biochim. Biophys. Acta* **1791,** 8–16
70. Desbarats, J., Birge, R. B., Mimouni-Rongy, M., Weinstein, D. E., Palerme, J. S., and Newell, M. K. (2003) *Nat. Cell Biol.* **5,** 118–125
71. Bordt, S. L., McKeon, R. M., Li, P. K., Witt-Enderby, P. A., and Melan, M. A. (2001) *Biochim. Biophys. Acta* **1499,** 257–264
72. Barnes, A. P., Solecki, D., and Polleux, F. (2008) *Curr. Opin. Neurobiol.* **18,** 44–52
73. Piper, M., van Horck, F., and Holt, C. (2007) *Adv. Exp. Med. Biol.* **621,** 134–143
74. Shelly, M., Cancedda, L., Heilshorn, S., Sumbre, G., and Poo, M. M. (2007) *Cell* **129,** 565–577
75. Hollis, E. R., 2nd, Jamshidi, P., Löw, K., Blesch, A., and Tuszynski, M. H. (2009) *Proc. Natl. Acad. Sci. U.S.A.* **106,** 7215–7220
76. Nakata, H. (2007) *Biochem. Biophys. Res. Commun.* **355,** 842–848
77. Dimitropoulou, A., and Bixby, J. L. (2000) *Brain Res* **858,** 205–214
78. Perron, J. C., and Bixby, J. L. (1999) *Mol. Cell. Neurosci.* **13,** 362–378
79. Kushner, S. A., Elgersma, Y., Murphy, G. G., Jaarsma, D., van Woerden, G. M., Hojjati, M. R., Cui, Y., LeBoutillier, J. C., Marrone, D. F., Choi, E. S., De Zeeuw, C. I., Petit, T. L., Pozzo-Miller, L., and Silva, A. J. (2005) *J. Neurosci.* **25,** 9721–9734
80. Elowe, S., Holland, S. J., Kulkarni, S., and Pawson, T. (2001) *Mol. Cell. Biol.* **21,** 7429–7441
81. Perlson, E., Hanz, S., Ben-Yaakov, K., Segal-Ruder, Y., Seger, R., and Fainzilber, M. (2005) *Neuron* **45,** 715–726
82. Lin, Y. H., Park, Z. Y., Lin, D., Brahmbhatt, A. A., Rio, M. C., Yates, J. R., 3rd, and Klemke, R. L. (2004) *J. Cell Biol.* **165,** 421–432
83. Chodniewicz, D., and Klemke, R. L. (2004) *Exp. Cell Res.* **301,** 31–37
84. Chodniewicz, D., and Klemke, R. L. (2004) *Biochim. Biophys. Acta* **1692,** 63–76
85. Kain, K. H., and Klemke, R. L. (2001) *J. Biol. Chem.* **276,** 16185–16192
86. Darenfed, H., Dayanandan, B., Zhang, T., Hsieh, S. H., Fournier, A. E., and Mandato, C. A. (2007) *Cell Motil. Cytoskeleton* **64,** 97–109
87. Zhang, X. F., Schaefer, A. W., Burnette, D. T., Schoonderwoert, V. T., and Forscher, P. (2003) *Neuron* **40,** 931–944
88. Narumiya, S., Ishizaki, T., and Uehata, M. (2000) *Methods Enzymol.* **325,** 273–284
89. Kao, H. T., Song, H. J., Porton, B., Ming, G. L., Hoh, J., Abraham, M., Czernik, A. J., Pieribone, V. A., Poo, M. M., and Greengard, P. (2002) *Nat. Neurosci.* **5,** 431–437
90. Vaudry, D., Stork, P. J., Lazarovici, P., and Eiden, L. E. (2002) *Science* **296,** 1648–1649
91. Maina, F., Hilton, M. C., Ponzetto, C., Davies, A. M., and Klein, R. (1997) *Genes Dev.* **11,** 3341–3350
92. Suetsugu, S., Hattori, M., Miki, H., Tezuka, T., Yamamoto, T., Mikoshiba, K., and Takenawa, T. (2002) *Dev. Cell* **3,** 645–658
93. Paglini, G., and Cáceres, A. (2001) *Eur. J. Biochem.* **268,** 1528–1533
94. Yoshimura, T., Kawano, Y., Arimura, N., Kawabata, S., Kikuchi, A., and Kaibuchi, K. (2005) *Cell* **120,** 137–149
95. Haeusgen, W., Boehm, R., Zhao, Y., Herdegen, T., and Waetzig, V. (2009) *Neuroscience* **161,** 951–959
96. Yang, Y. C., Lin, C. H., and Lee, E. H. (2006) *Mol. Cell. Biol.* **26,** 8357–8370
97. Pouysségur, J., Volmat, V., and Lenormand, P. (2002) *Biochem. Pharmacol* **64,** 755–763
98. Howe, A. K., Aplin, A. E., and Juliano, R. L. (2002) *Curr. Opin. Genet. Dev.* **12,** 30–35
99. McLeod, S. J., Shum, A. J., Lee, R. L., Takei, F., and Gold, M. R. (2004) *J. Biol. Chem.* **279,** 12009–12019
100. Enserink, J. M., Price, L. S., Methi, T., Mahic, M., Sonnenberg, A., Bos, J. L., and Taskén, K. (2004) *J. Biol. Chem.* **279,** 44889–44896
101. Kinbara, K., Goldfinger, L. E., Hansen, M., Chou, F. L., and Ginsberg, M. H. (2003) *Nat. Rev. Mol. Cell Biol.* **4,** 767–776

102. Retta, S. F., Balzac, F., and Avolio, M. (2006) *Eur J. Cell Biol.* **85,** 283–293
103. Alessandrini, A., Greulich, H., Huang, W., and Erikson, R. L. (1996) *J. Biol. Chem.* **271,** 31612–31618
104. Pham, C. D., Arlinghaus, R. B., Zheng, C. F., Guan, K. L., and Singh, B. (1995) *Oncogene* **10,** 1683–1688
105. Gerits, N., Kostenko, S., Shiryaev, A., Johannessen, M., and Moens, U. (2008) *Cell. Signal.* **20,** 1592–1607
106. Dhillon, A. S., Meikle, S., Peyssonnaux, C., Grindlay, J., Kaiser, C., Steen, H., Shaw, P. E., Mischak, H., Eychène, A., and Kolch, W. (2003) *Mol. Cell. Biol.* **23,** 1983–1993
107. Halpain, S., and Dehmelt, L. (2006) *Genome Biol.* **7,** 224
108. Arimura, N., Ménager, C., Kawano, Y., Yoshimura, T., Kawabata, S., Hattori, A., Fukata, Y., Amano, M., Goshima, Y., Inagaki, M., Morone, N., Usukura, J., and Kaibuchi, K. (2005) *Mol. Cell. Biol.* **25,** 9973–9984
109. Inagaki, N., Chihara, K., Arimura, N., Ménager, C., Kawano, Y., Matsuo, N., Nishimura, T., Amano, M., and Kaibuchi, K. (2001) *Nat. Neurosci.* **4,** 781–782
110. Arimura, N., Inagaki, N., Chihara, K., Ménager, C., Nakamura, N., Amano, M., Iwamatsu, A., Goshima, Y., and Kaibuchi, K. (2000) *J. Biol. Chem.* **275,** 23973–23980
111. Lanier, L. M., and Gertler, F. B. (2000) *Curr. Opin. Neurobiol.* **10,** 80–87
112. Hernández, S. E., Settleman, J., and Koleske, A. J. (2004) *Curr. Biol.* **14,** 691–696
113. Huang, J., Sakai, R., and Furuichi, T. (2006) *Mol. Biol. Cell* **17,** 3187–3196
114. Ehler, E., van Leeuwen, F., Collard, J. G., and Salinas, P. C. (1997) *Mol. Cell. Neurosci.* **9,** 1–12
115. Mavria, G., Vercoulen, Y., Yeo, M., Paterson, H., Karasarides, M., Marais, R., Bird, D., and Marshall, C. J. (2006) *Cancer Cell* **9,** 33–44
116. Ehrenreiter, K., Piazzolla, D., Velamoor, V., Sobczak, I., Small, J. V., Takeda, J., Leung, T., and Baccarini, M. (2005) *J. Cell Biol.* **168,** 955–964
117. Stork, P. J., and Schmitt, J. M. (2002) *Trends Cell Biol.* **12,** 258–266